Balancing of a Planar Bouncing Object

Nina B. Zumel

CMU-RI-TR-93-26

The Robotics Institute
Carnegie Mellon University
Pittsburgh, PA 15213

Abstract

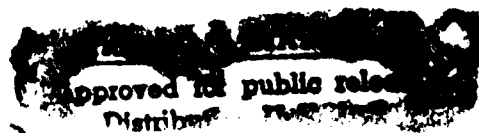While most previous work in planning manipulation tasks has relied on the assumption of quasi-static conditions, there can be situations where the quasi-static assumption may not hold, and the assumptions about the environment must be relaxed. This is true, for example, in a situation where objects are making and breaking contact at high enough velocities that contact dynamics play a significant effect in the motion of the colliding objects.

There has been some work studying models of collision, in particular for the design and analysis of systems with intermittent constraints, and for the design of juggling robots. Our work extends previous studies in planar juggling to the case of a polygonal object, using the model of rigid body impulsive collision. Simulations verify the results of a linearized analysis.

Contents

List of Figures

List of Tables

5

1 Motivation

Most previous strategies for planning manipulation tasks have relied on an assumption of quasi-static mechanics in the analysis of the physical system. This constrains the plans to situations that are slow moving, and in which contact dynamics can be neglected.

One can imagine situations these assumptions do not hold or when a model of the contact dynamics would be useful. In catching an already moving or accelerating object, for instance, the inertial properties of the object affect the motion which results from the applied forces of collision. Knowledge of the magnitudes as well as the direction of forces and velocities becomes important. Juggling and table tennis are two such domains that have been explored in robotics. Catching of tossed objects is a related task in which such knowledge is useful.

Another domain in which such a model may be useful is in the manipulation of objects by sliding on a frictional support surface. Much work has been done in the analysis of quasistatic pushing in the presence of friction ([13], [12], [14]). [8] shows that the motion of an object on a frictional support surface can be determined if the pressure distribution of the object is known. [12] and [14] analyze this situation when the pressure distribution is not known. The analysis of [8] implies that for large enough applied forces, the motion of the object is essentially given by the acceleration due to the applied forces. Since the impact model assumes that at the moment of collision the impact force "swamps out" all other forces, the use of controlled collision can be useful in situations where the pressure distribution is not completely known, particularly if the support friction is fairly low.

Some work has been done to study models of dynamic collision for use in robotic domains. [15] designed a dynamically stable hopping robot, modelling the bounce as a spring and damper system with perfectly inelastic collision. This system was further analyzed by [9]. [1] designed a ping-pong playing robot which used a simple model of point-mass collision to predict the motion of the ball after striking. [19] attempts to characterize the qualitative behavior change in the motion of objects upon collision. [20] simulates and analyzes systems with intermittent constraints, and uses models of those systems in planning manipulation tasks. [5] analyses and designs a planar puck juggling system. [16] extends this to the 3-D case. This work continues those studies, extending the planar puck juggling work of [5] to objects with extent and orientation. The intent is to evaluate the utility of the impact model for manipulation planning.

2 The Problem

We have a planar object on a frictionless inclined plane, pulled by the influence of gravity down to a movable "table", against which it bounces with coefficient
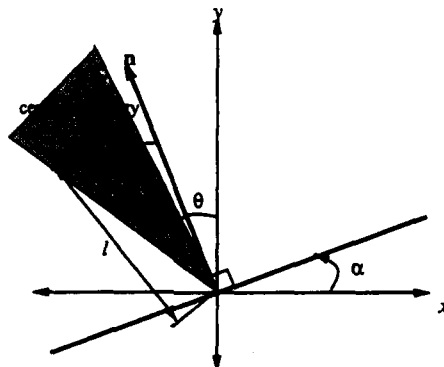
7

Figure 1: Basic System Geometry

of restitution e. The coefficient of friction between table and object is μ. The contact between the table and the object is a point contact, at a known point on the object. We assume an impulsive impact model as described by [17] and used by [19], [20].

The object is parameterized by $(x, y, \rho\theta)$, where (x, y) are the coordinates of the center of gravity of the object, θ is the orientation of the object, and ρ is the radius of gyration of the object ([6]). The desired orientation of the object will be set to $\theta = 0$. For simplicity, we can abstract away the dimensions of the actual object, and think of the object as a rod, whose center of gravity is the center of gravity of the object, located at length l from the from the contact point[1] (See figure 1). We want to have the object bouncing to a fixed height while maintaining the desired orientation. Ideally, we would prefer the bouncing to occur in a fixed (impact) position in the ¡x y¿ plane, but we will initially disregard this constraint, and study the simpler, lower dimensional unconstrained case.

In this examination, we will also assume perfect sensing and perfect control of the motion of the table, for the purpose of examining the question of whether the desired behavior is achievable in theory, before exploring problems in actual implementation.

2.1 The Lossless Case

We first look at the simplest case, the case $e = 1, \mu = 0$. In this case, the equation describing the change in velocity due to an impulsive collision can be

---

[1] This of course ignores the question of whether or not we can actually strike the object at the angle desired at exactly the point desired, so in effect we are assuming the object is "pointy enough" at the contact point.

written in terms of the preimpact velocity $\mathbf{v}^-$ as

$$\Delta\mathbf{v} = -2(\hat{\mathbf{n}}^T\mathbf{v}^-)\hat{\mathbf{n}} \tag{1}$$

(see Appendix A), where

$$\hat{\mathbf{n}} = \frac{\rho}{\sqrt{\rho^2 + l^2\sin^2\beta}} \begin{bmatrix} -\sin\alpha \\ \cos\alpha \\ \frac{l}{\rho}\sin\beta \end{bmatrix}. \tag{2}$$

As shown in Figure 1, α is the angle that the table makes with the horizontal in the counterclockwise direction, l is the length from the center of gravity to the contact point, and β is the angle that l makes with the table normal in the counterclockwise direction. Note that $\beta = \theta - \alpha$.

Equation (1) simply says that in configuration space, the object upon impact will reverse its normal velocity component while its tangential component remains unchanged. Define the constraint surface to be the set of configurations for which the object touches the table without penetration for a given table orientation, α (see [11] for a discussion of configuration space). Then according to equation (1), the object will reflect about the normal to the constraint surface. This is a fairly intuitive extension of the usual example of a perfectly elastic, frictionless point mass impact against a flat barrier.

In order to get some idea of possible solutions to our original problem, we can first look at the case of this point mass bouncing against our table. If the ball makes impact with a horizontal ($\alpha = 0$) table with a velocity vector at angle $\beta = \theta$ with the vertical, it will leave after impact with angle $-\theta$, fall under the influence of gravity, and then (if the table remains at the same height) strike the table again at angle θ. We would like to control the strikes so that θ eventually goes to zero, and the ball bounces straight up and down. One way to do this is tilt the table while simultaneously moving it so that impact always occurs at a given height in the vertical plane, say $y = 0$.

Suppose, as in figure 3, that the ball first makes impact with velocity at angle θ^- to the vertical. If the table is tilted at angle α at impact, the ball will leave the table at angle $-\beta = -(\theta^- - \alpha)$, which is equivalent to angle $-\theta^- + 2\alpha$ to the vertical. Hence, on the next impact, it will strike with the negative of that angle with respect to the vertical. This gives the system equation

$$\theta_{n+1} = \theta_n - 2\alpha_n \tag{3}$$

where θ_n gives the velocity angle with respect to the vertical just before the the nth impact. If we choose α to be proportional to θ, say $\alpha = \kappa\theta$, the recurrence relation becomes

$$\theta_{n+1} = (1 - 2\kappa)\theta_n \tag{4}$$

or

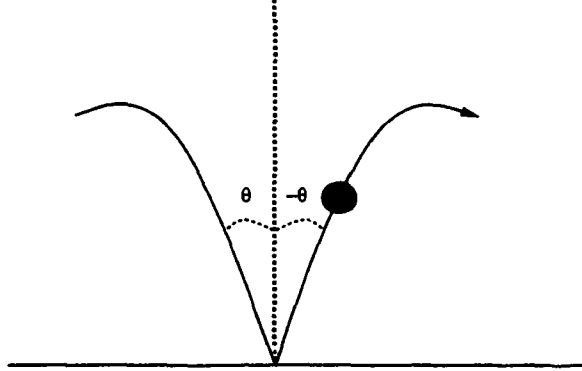$$\theta_n = (1 - 2\kappa)^n\theta_0. \tag{5}$$

9

Figure 2: Bouncing Ball example

This will eventually drive the system to its equilibrium state, $\theta = 0$, as long as $|1 - 2\kappa| < 1$, or $0 < \kappa < 1$. We can try to extend this strategy to the rigid body case.

2.1.1 System Equations

We can rewrite equation 1 in the form

$$\mathbf{v}^+ = (\mathbf{I} - 2\hat{\mathbf{n}}\hat{\mathbf{n}}^T)\mathbf{v}^- \tag{6}$$

where $\mathbf{v}^-$ is the velocity vector immediately before impact, $\mathbf{v}^+$ is the velocity immediately after impact, and $\mathbf{I}$ is the identity matrix. After impact, during the ballistic phase, we have the equations

$$
\begin{aligned}
\dot{x}(t) &= \dot{x}_0 \\
\dot{y}(t) &= \dot{y}_0 - Gt \\
\rho\dot{\theta}(t) &= \rho\dot{\theta}_0
\end{aligned}
\tag{7}
$$

where the subscripted velocities are the velocities at the beginning of the ballistic phase, $i.e.$ the velocities given by $\mathbf{v}^+$. G is the acceleration of gravity. The next impact occurs at $y_{contact} = 0$, when the contact condition

$$l\cos\theta_0 + \dot{y}_0 t - \frac{1}{2}Gt^2 = l\cos(\theta_0 + \dot{\theta}_0 t) \tag{8}$$

is satisfied. The time until next impact is a function of θ_0, $\dot{\theta}_0$, and $\dot{y}_0$, which in turn are functions of the configuration just prior to impact, $(\theta^-, \mathbf{v}^-)$. Let the configuration at impact n be given by $\mathbf{x}_n = (\rho\theta, \dot{x}, \dot{y}, \rho\dot{\theta})_n$, and call the time of next impact $\tau(\mathbf{x}_n)$. Then the impact equations plus the contact condition
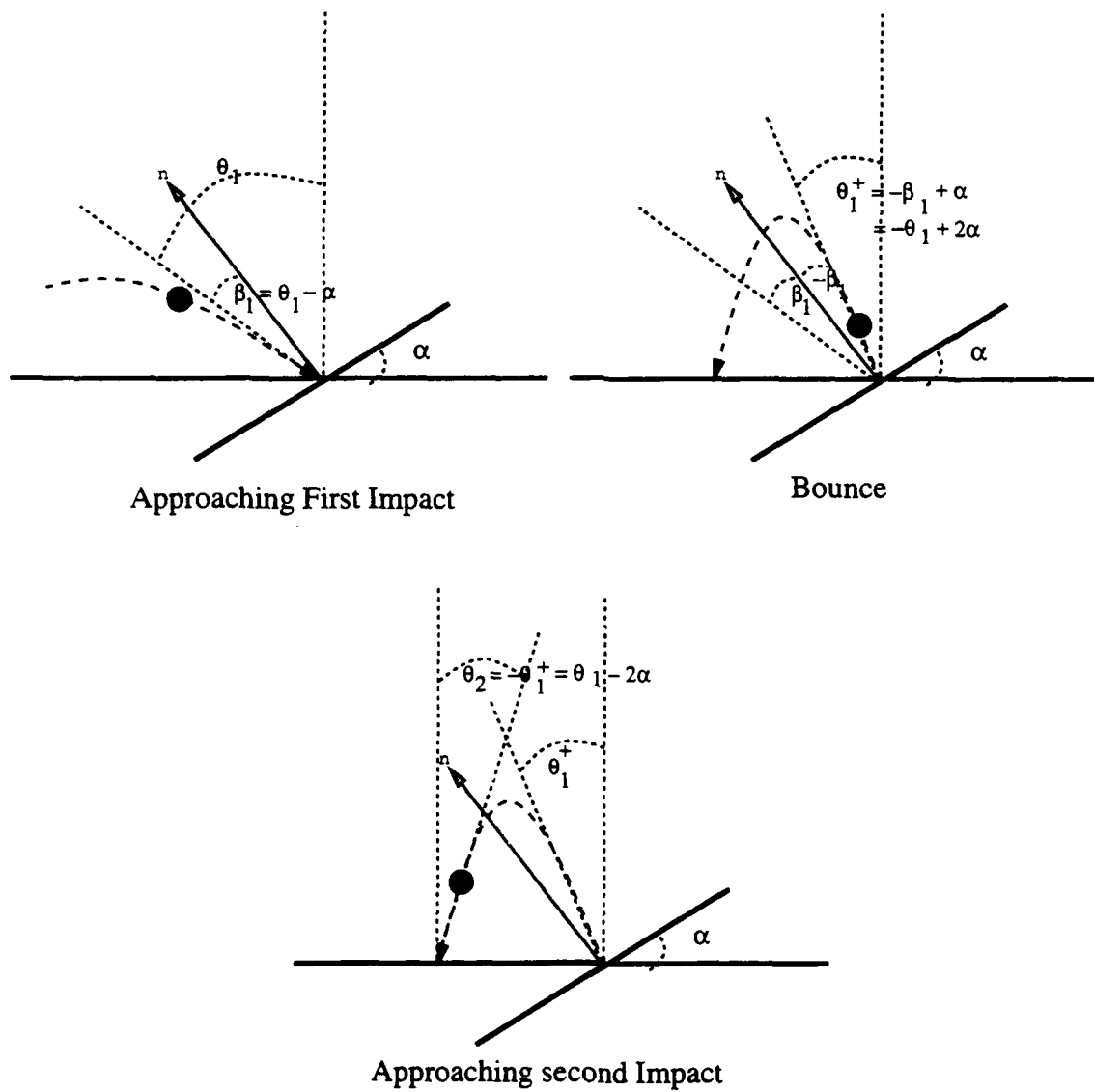
10

Figure 3: Ball bouncing against tilted table

describe a nonlinear recurrence relation,

$$\mathbf{x}_{n+1} = \mathbf{f}(\alpha, \mathbf{x}_n, \tau(\mathbf{x}_n)). \tag{9}$$

If we set $\alpha = \kappa\theta$, then $\mathbf{f}$ is completely a function of $\mathbf{x}_n$, and we can try to find a fixed point $\mathbf{x}^*$. By inspection of (6), (7), and (8), we can see that $(\theta = \dot{\theta} = 0, \dot{y} = \dot{y}^*, \dot{x} = \dot{x}^*)$ defines a set of fixed points, with $\tau = -2\dot{y}^*/G$. Further, we know that for a lossless system that the energy at contact, $\frac{1}{2}m(\dot{x}^2 + \dot{y}^2 + \rho^2\dot{\theta}^2) + mGl\cos\theta$, is constant from impact to impact, so our initial conditions determine the energy surface to which we are constrained. For specificity, we choose an equilibrium point from our set of possible fixed points to study. Since we would like our object to bounce in place horizontally, we choose $\dot{x}^* = 0$. Then, if we drop the object from a (center of gravity) height y_0, with a initial velocity vector $\mathbf{v}_0$, the corresponding value for $\dot{y}^*$ is given by

$$\dot{y}^* = -\sqrt{2G(y_0 - l\cos\theta) + \mathbf{v}_0^T\mathbf{v}_0}. \tag{10}$$

We wish to determine the stability of the state $\mathbf{x}^* = (0, 0, \dot{y}^*, 0)$: if we start off, not exactly at this point, but merely near it, can we balance the object?

2.1.2 Linearized Analysis

Given $\mathbf{x}^* = \mathbf{f}(\mathbf{x}^*)$ for the recurrence relation $\mathbf{x}_{n+1} = \mathbf{f}(\mathbf{x}_n)$, Taylor expansion about $\mathbf{x}^*$ gives us

$$\begin{aligned} \mathbf{f}(\mathbf{x}^* + \delta\mathbf{x}_n) &\simeq \mathbf{x}^* + \delta\mathbf{x}_{n+1} \\ &\simeq \mathbf{x}^* + \mathcal{J}(\mathbf{x}^*)\delta\mathbf{x}_n + h.o.t \end{aligned} \tag{11}$$

where $\mathcal{J}(\mathbf{x})$ is the Jacobian of $\mathbf{f}(\cdot)$ evaluated at $\mathbf{x}$. Ignoring higher order terms gives the approximate linear system

$$\delta\mathbf{x}_{n+1} \approx \mathcal{J}(\mathbf{x}^*)\delta\mathbf{x}_n, \tag{12}$$

or

$$\delta\mathbf{x}_n = [\mathcal{J}(\mathbf{x}^*)]^n \delta\mathbf{x}_0. \tag{13}$$

From the linearized systems, we can try to predict certain properties of the nonlinear system in the neighborhood of $\mathbf{x}^*$ (see Appendix B).

The linearized system around $\mathbf{x}^*$ is given by the system matrix

$$\mathcal{J} = \begin{bmatrix} 1 + \frac{4\dot{y}^{*2}(1-\kappa)l}{G\rho^2} & 0 & 0 & -\frac{2\dot{y}^*}{G} \\ \frac{2\dot{y}^*\kappa}{\rho} & 1 & 0 & 0 \\ 0 & 0 & 1 & 0 \\ \frac{2\dot{y}^*(\kappa-1)l}{\rho^2} & 0 & 0 & 1 \end{bmatrix} \tag{14}$$

12

which has eigenvalues λ_i given by

$$
\begin{aligned}
&1,\\
&1,\\
&\frac{2\ddot{y}^{*2}l(1-\kappa)+G\rho^2}{G\rho^2} \qquad\qquad \pm \qquad\qquad\\
&\qquad\qquad \frac{2\ddot{y}^*l\sqrt{\kappa-1}\sqrt{\ddot{y}^{*2}l(\kappa-1)-G\rho^2}}{G\rho^2},
\end{aligned}
\tag{15}
$$

If all the eigenvectors $\mathbf{V}_i$ are distinct, then the system solution is given by

$$
\delta\mathbf{x}_n = \sum_{i=1}^{4} c_i \mathbf{V}_i \lambda_i^{\,n},
\tag{16}
$$

the c_i being functions of the initial conditions. Clearly, in order for the solution to be stable, all the eigenvalues must be contained in the closed unit disc of the complex plane. Analyzing $\lambda_{3,4}$ for different values of κ gives

$$
\kappa < 1: \quad |\lambda_3| > 1, |\lambda_4| < 1 \quad \text{Unstable}
\tag{17}
$$

$$
1 < \kappa < 1 + \frac{G\rho^2}{\ddot{y}^{*2}l}: \quad |\lambda_{3,4}| = 1 \qquad \text{Stable}
\tag{18}
$$

$$
\kappa > 1 + \frac{G\rho^2}{\ddot{y}^{*2}l}: \quad |\lambda_3| < 1, |\lambda_4| > 1 \quad \text{Unstable}.
\tag{19}
$$

The boundaries of the region given by (18) are special cases, because for those values of κ not all the eigenvectors are distinct, and the analysis is more complicated (see Appendix C). For the region of stable κ, (16) can be written in the form

$$
\delta\mathbf{x}_n = c_1
\begin{bmatrix} 0 \\ 1 \\ 0 \\ 0 \end{bmatrix}
+ c_2
\begin{bmatrix} 0 \\ 0 \\ 1 \\ 0 \end{bmatrix}
+ 2\mathrm{Re}\left(c_3 e^{j\sigma n}
\begin{bmatrix} a+jb \\ g \\ 0 \\ h \end{bmatrix}
\right),
\tag{20}
$$
$$
\sigma, a, b, g, h \in \Re
$$

and the initial conditions give for the constants of proportionality:

$$
c_1 = \delta\dot{x}_0 - \frac{\rho\delta\dot{\theta}_0}{h}g,
\tag{21}
$$

$$
c_2 = \delta\dot{y}_0,
\tag{22}
$$

$$
c_3 = \frac{\rho\delta\dot{\theta}_0}{2h} + j\left(\frac{a\rho\delta\dot{\theta}_0}{2bh} - \frac{\rho\delta\theta_0}{2b}\right).
\tag{23}
$$

The linear analysis predicts that in the neighborhood about the equilibrium point, if there is any deviation from $\ddot{y}^*$, it will stay constant; if $\delta\dot{x}_0 = 0$ and

13

	θ_0 [rad]	$\dot{\theta}_0$ [rad/s]	y_0 [m]	κ	$\kappa_{critical}$
Case 1	0.3	0	0.2	1.1	1.5
Case 2	0	0.1	0.2	1.1	1.5
Case 3	0.1	0	0.2	1.55	1.5

Table 1: Cases simulated for Lossless System. $\dot{x}_0 = 0$ and $\dot{y} = 0$ when object was dropped.

$\delta\dot{\theta}_0 = 0$, then $\delta\dot{x}, \delta\theta$, and $\delta\dot{\theta}$ will all oscillate about the origin at frequency σ, with amplitudes determined by $\delta\theta_0$. These, then, are the initial conditions that determine the stability of $\mathbf{x}^*$. If either $\delta\dot{x}_0$ or $\delta\dot{\theta}_0$ are nonzero, there will be a net x velocity, and the object will remain balanced, but travel horizontally as it bounces. Strictly speaking, this is not really stable, since x (which we have been ignoring up until now) can increase without bound. But since $\mathbf{x}^*$ does not contain x, it does remain bounded. For the case $\kappa = \kappa_{critical} = 1 + (G\rho^2)/(\dot{y}^{*2}l)$, linear analysis predicts instability of the system (see Appendix C).

2.1.3 Empirical Verification

Simulation showed that the linear approximation predicted the stability of the system reasonably well for different choices of κ: the region described by (18) was indeed stable for small initial velocities and for angular deviations up to about ± 0.4 radians ($\approx 23°$). When the initial impact angle was small, about ± 0.15 radians ($\approx 8.6°$) or less, the system was stable all the way up to and including $\kappa = \kappa_{critical}$. When the initial impact angle was about in the range $\pm(0.15$ to $0.4)$ radians, κ had to be much closer to unity for stability. The $\kappa = 1$ case is always unstable, but the $\kappa = \kappa_{critical}$ case can be stable, despite the linear prediction. Note for comparison that the range ± 0.5 radians ($\approx 30°$), is the range over which the linear approximation $\sin x \approx x$ holds.

All examples shown are for simulations of an isosceles triangle of uniform mass distribution, 10 centimeters wide at the base, and 20 centimeters high. The radius of gyration about the center of gravity for this triangle is about 9.428 centimeters.

The figures for cases 1 and 2, which were stable, show projections of the system orbit in the $< \theta \; \dot{\theta} >$ plane (θ is on the horizontal axis) and the projection in the $< \dot{x} \; \dot{y} >$ plane. Notice in Figures 5 and 6 that the $< \theta \; \dot{\theta} >$ projection is centered about the origin in both cases, showing that θ and $\dot{\theta}$ oscillate about zero. In case 1 (Figure 5), where there were no initial velocities (when the object was dropped), $\dot{x}$ is also centered about the origin, and $\dot{y}$ is bounded in the neighborhood of $\dot{y}_0$, the y-velocity at first impact. In case 2 (Figure 6), where there was some initial angular rotation, $\dot{x}$ is no longer centered about zero. Case 3 (Figure 7), where $\kappa > \kappa_{critical}$, was unstable, and the curve in the $< \theta \; \dot{\theta} >$ plane eventually goes unbounded.

14
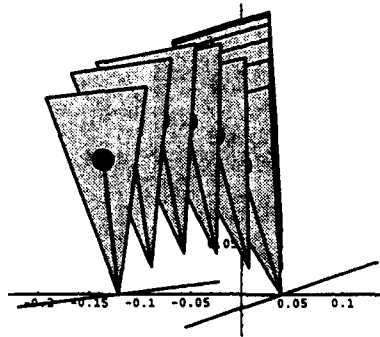
Figure 4: Simulated system

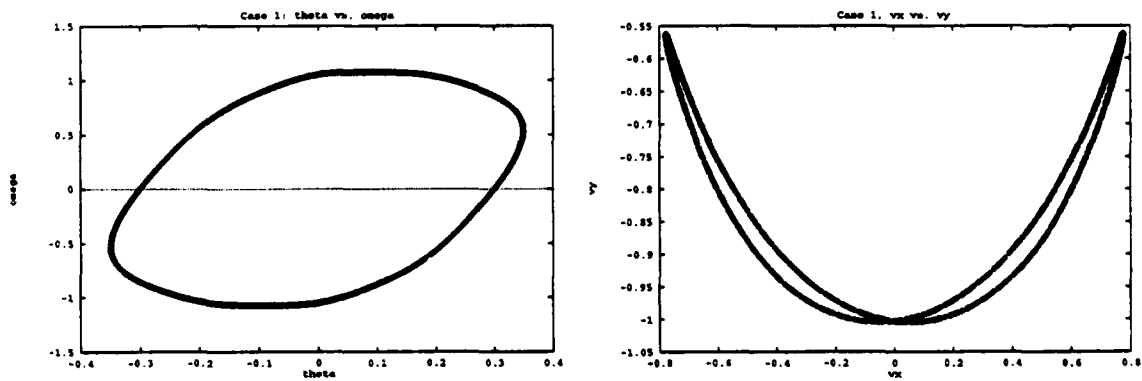
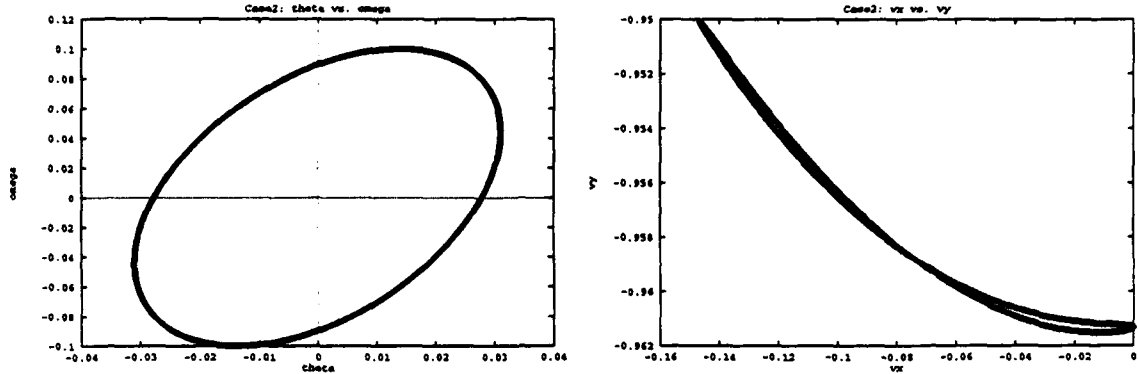Figure 5: Lossless case1 with $\theta_0 = 0.3$rad, $\dot{\theta}_0 = 0$rad/s, $\kappa = 1.1$

15

Figure 6: Lossless case 2 with $\theta_0 = 0\text{rad}, \dot{\theta}_0 = 0.2\text{rad/s}, \kappa = 1.1$

2.2 Extensions to More General Cases

We can extend the above analysis in order to generalize the lossless case.

2.2.1 Inelastic collision

For the case $e \neq 1$ we can simulate the lossless case by giving velocity to the table; if we assume that $mass_{table} \gg mass_{object}$, then

$$\mathbf{v}^+ = (\mathbf{I} - (1+e)\hat{\mathbf{n}}\hat{\mathbf{n}}^T)\mathbf{v}^- + (1+e)\hat{\mathbf{n}}\hat{\mathbf{n}}^T\mathbf{v}_{table} \qquad (24)$$

(see Appendix A) and $\mathbf{v}_{table}$ remains unchanged due to our assumption about the relative masses. If we set

$$\mathbf{v}_{table} = -\frac{1-e}{1+e}\mathbf{v}^-, \qquad (25)$$

then (24) reduces to the equation for the lossless case. This choice of $\mathbf{v}_{table}$ can be thought of as having the table tracking the orientation of the object and the velocity of the contact point, and striking the object with the table oriented at angle α, and moving in its normal direction at the appropriate speed. This can be seen by noting that

$$
\begin{aligned}
\dot{x}_{contact} &= \dot{x} + l\dot{\theta}\cos\theta \\
\dot{y}_{contact} &= \dot{y} + l\dot{\theta}\sin\theta,
\end{aligned}
\qquad (26)
$$

when measured in the global frame (corresponding to $\alpha = 0$). Then another choice for $\mathbf{v}_{table}$ that will give the same system equations as (25) is

$$\mathbf{v}_{table} = -\frac{1-e}{1+e}\hat{\mathbf{n}}\hat{\mathbf{n}}^T \begin{bmatrix} \dot{x}_{contact} \\ \dot{y}_{contact} \\ 0 \end{bmatrix} \qquad (27)$$
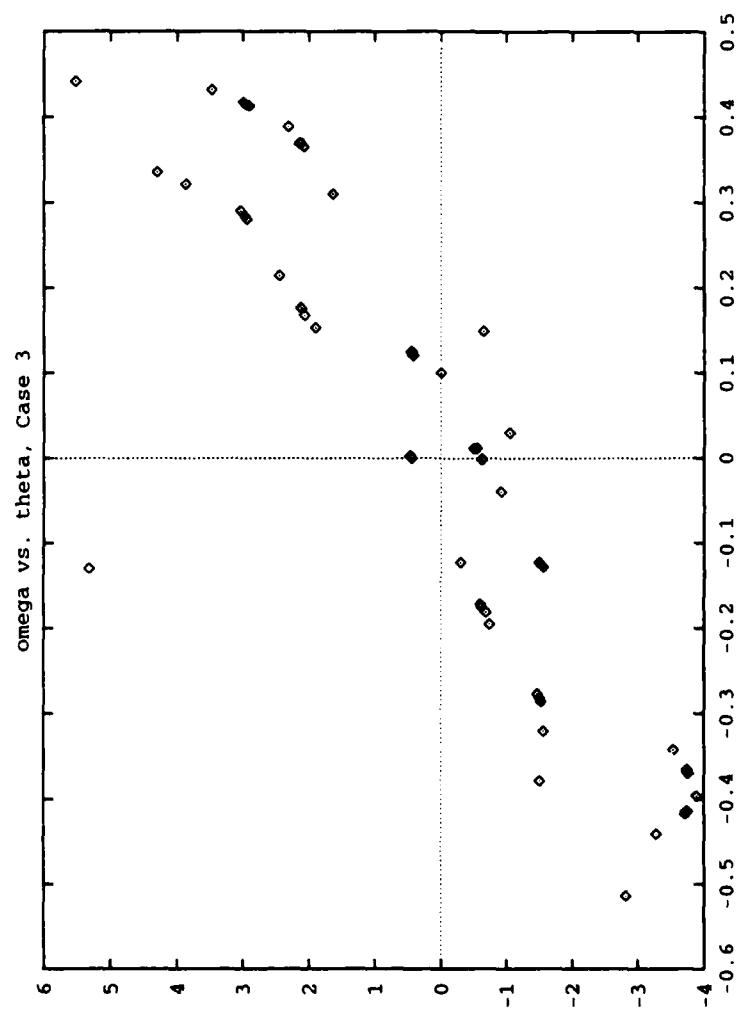
16

Figure 7: Unstable case: $\kappa > \kappa_{critical}$

17

	θ_0 [rad]	$\dot{\theta}_0$ [rad/s]	y_0 [m]	y^* [m]	$\dot{y}^*$ [m/s]	κ	$\kappa_{critical}$	κ_E	$E_{desired}$ [Nm]
Case 4	0.3	0	0.2	0.25	-1.27	1.1	1.28	0.165	1.73
Case 5	0	0.1	0.2	0.25	-1.27	1.1	1.28	0.165	1.73

Table 2: Cases simulated for system with energy feedback. $e = 0.5$

2.2.2 Energy Feedback

If in addition to having the object bounce straight up and down, one also wanted the object to bounce to a specific (center of gravity) height, y^*, the associated (unit mass) energy level $\eta^* = Gy^*$ can be used as an additional feedback term. As in [5], we can use the feedback law

$$
\begin{aligned}
\mathbf{v}_{table} &= -\left[\tfrac{1-e}{1+e} + \kappa_E(\eta^* - \eta)\right] \mathbf{v}_{contact}, \\
\eta^* &= Gy^* \\
&= Gl + \tfrac{1}{2}\dot{y}^{*2}, & \text{at impact} \\
\eta &= Gl\cos\theta + \tfrac{1}{2}\dot{y}^2 & \text{at impact.}
\end{aligned}
\tag{28}
$$

For stability, κ_E should be in the range $0 < \kappa_E < \frac{4}{(1+e)\dot{y}^{*2}} \doteq \kappa_{Emax}$ ([5]). α still is set to $\kappa\theta$, and the new critical value for κ is now

$$
\kappa_{critical} = 1 + \frac{2G\rho^2}{(1+e)\dot{y}^{*2}l}.
\tag{29}
$$

The eigenvectors and eigenvalues of the linearized system are essentially the same (for $0 < \kappa < \kappa_{critical}$), except the eigenvalue corresponding to the eigenvector $[0\ 0\ 1\ 0]^T$ (which is the eigenvector corresponding to $\delta\dot{y}$) is now given by the value $(1 - \frac{\kappa_E}{\kappa_{Emax}}) < 1$, reflecting the linearized prediction that the deviation in $\dot{y}$ goes to zero, i.e. that the system will converge to the correct energy surface[2]. Experiments confirm that for low values of κ_E (about $0.1\kappa_{Emax}$) the energy does indeed converge to the correct level (as seen in Figures 8 and 9 for cases 4 and 5), and then the behavior of the system is similar to the lossless case. For values of κ_E much higher than $0.1\kappa_{Emax}$, the system is generally unstable.

2.2.3 Friction

If we remove the assumption that $\mu_{table} = 0$, the impact equations become nonlinear, reflecting the nonlinearity of Coulomb friction. Although the analytic approach becomes more difficult, empirical studies for various values of μ found this case to be unstable when using the table tilt rule explained above, somewhat

---

[2]Strictly speaking, because this is no longer a lossless system, the fact that three of the eigenvalues are on the unit circle means we cannot use the linearized system to rigorously prove anything about the nonlinear system (see Appendix B), although [5] does present some complicated stability arguments for the point mass case. We can also use intuition, our knowledge about the lossless case, and empirical evidence to help us.
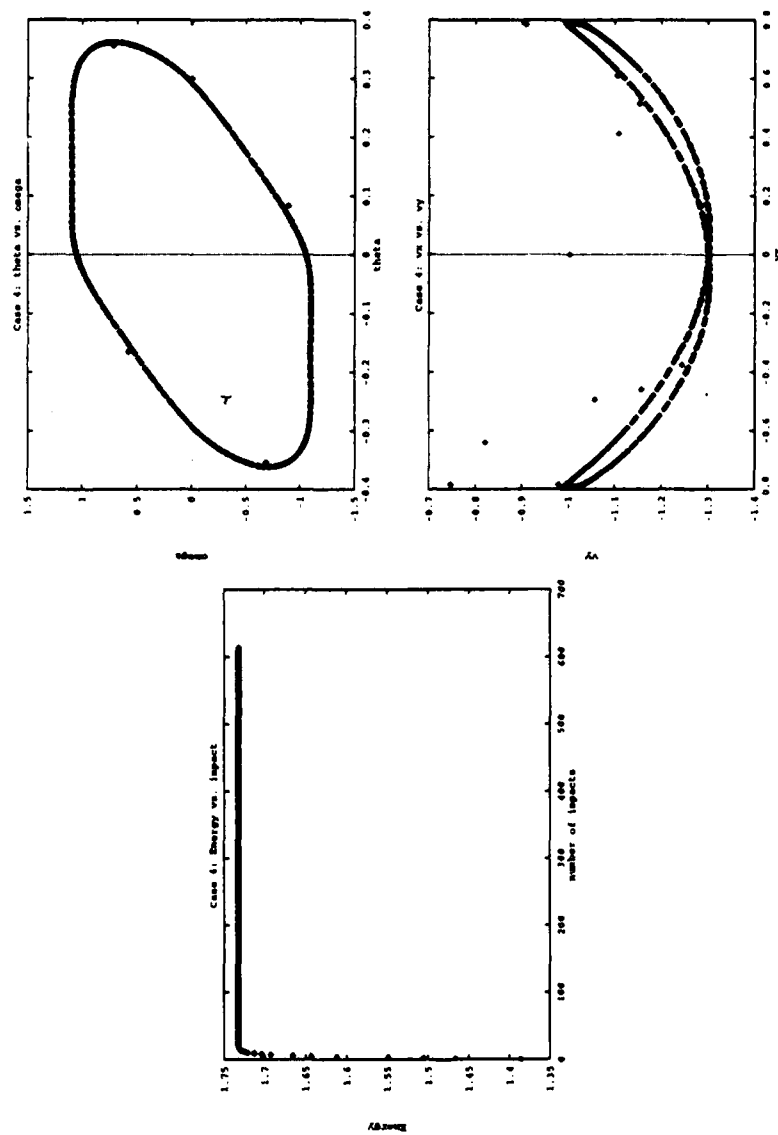
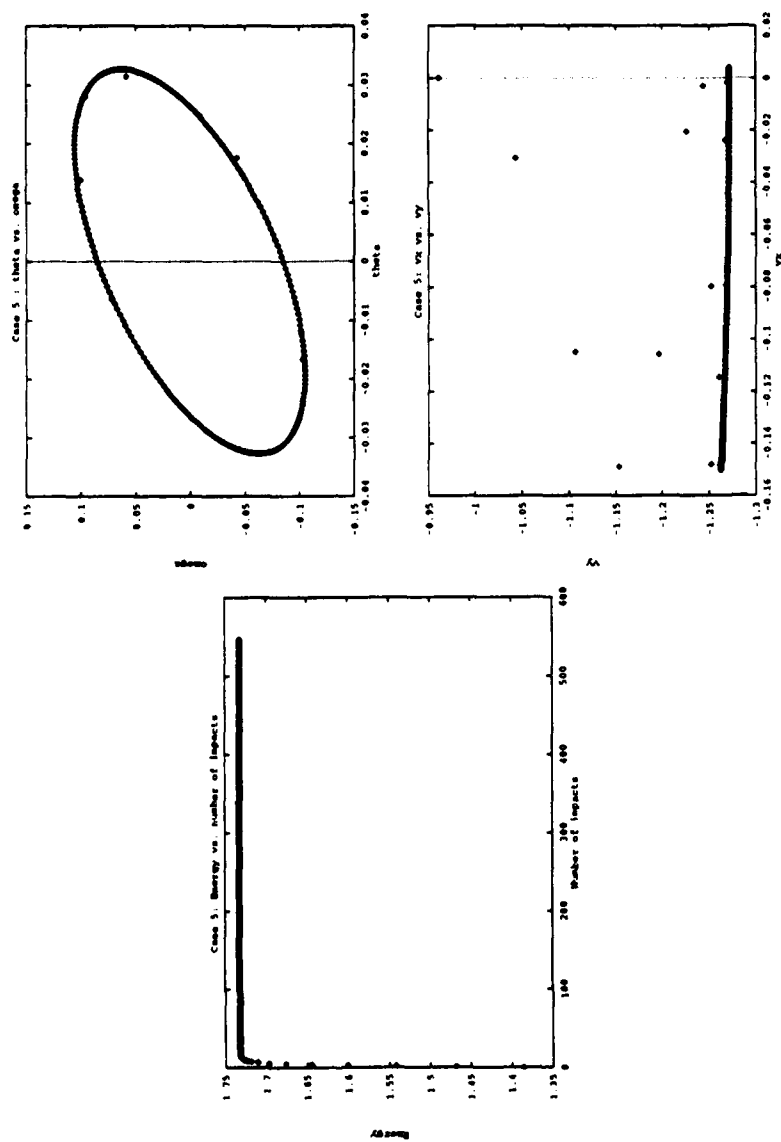Figure 8: Case 4:$\theta_0 = 0.3$rad, $e = 0.5$, $\kappa = 1.1$, $\kappa_E = 0.165$

Figure 9: Case 5: $\dot{\theta}_0 = 0.1\text{rad/s}, e = 0.5, \kappa = 1.1, \kappa_E = 0.165$
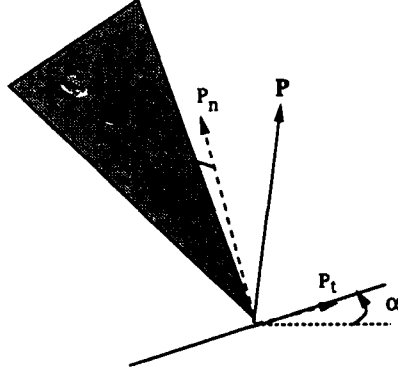
20

Figure 10: Tangential and Normal Impulses

contrary to expectations. Apparently, the law cannot compensate for the energy lost in the tangential direction, and in fact often added an impulse in a direction that increased θ, contributing to the tip-over of the object. This can be seen by looking at the equation for the moment due to the impulse (see figure (10))

$$
\begin{aligned}
M &= P_n l \sin \beta + P_t l \cos \beta \\
&= P_n l \sin \beta + \mu P_n \text{sgn} - v_{tc} l \cos \beta
\end{aligned}
\tag{30}
$$

for the case of sliding contact. Here P_t, P_n are the tangential and normal components of the contact, and $v_t c$ is the tangential contact velocity. For small angles, $\sin \beta \approx \beta$ and $\cos \beta \approx 1 - \beta^2 >> \beta$, so when β is smaller than μ, the moment due to frictional forces can potentially cancel out the desired moment, and cause the object to rotate in the wrong direction. This problem can be compensated for somewhat by increasing κ, which in general causes β to be larger. Increasing κ_E also prolongs the time that the object can be kept upright, but the tangential forces increase the horizontal motion of the object, and hence the energy dissipated to friction, and eventually the object falls over. This difficulty can probably be circumvented by striking the object at an angle that minimizes tangential velocity, or by striking at a different place. Neither of these options has been explored as yet, since both apparently require that more attention be paid to the actual dimensions of the object.

2.2.4 Imperfect Sensing and Control

Although the system has only been simulated, not actually built, an attempt was made to approximate imperfections in sensing and control by adding some Gaussian noise to the calculation of impact time used by the table. This changes the angle and velocity of the table at impact time, as well as the y-height at which contact is made. Zero mean gaussian noise with a standard deviation of 10

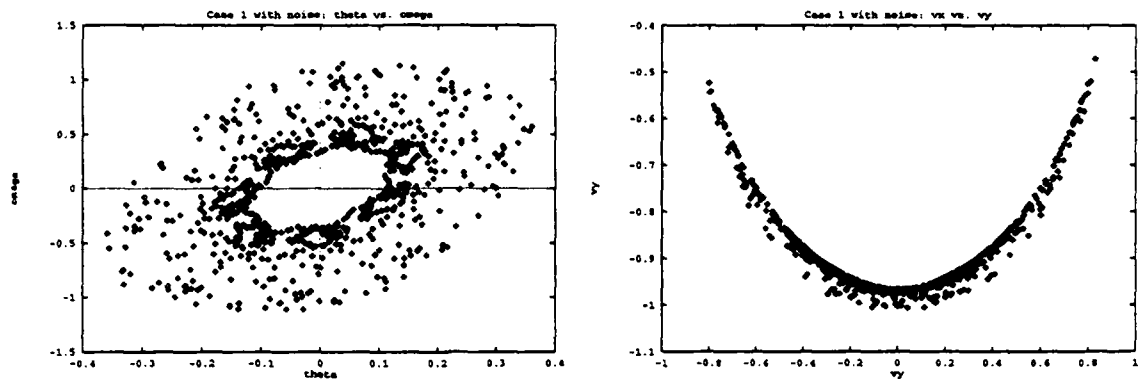Figure 11: Case 1 with noise

ms., which is about an order of magnitude less than the time between collisions, was used. Although the motion of the object with noise added appears much less smooth, the system remains stable in a similar range of initial conditions as the noiseless case. Cases 1 and 4 were resimulated, this time with noise, and shown in Figures 11 and 12.
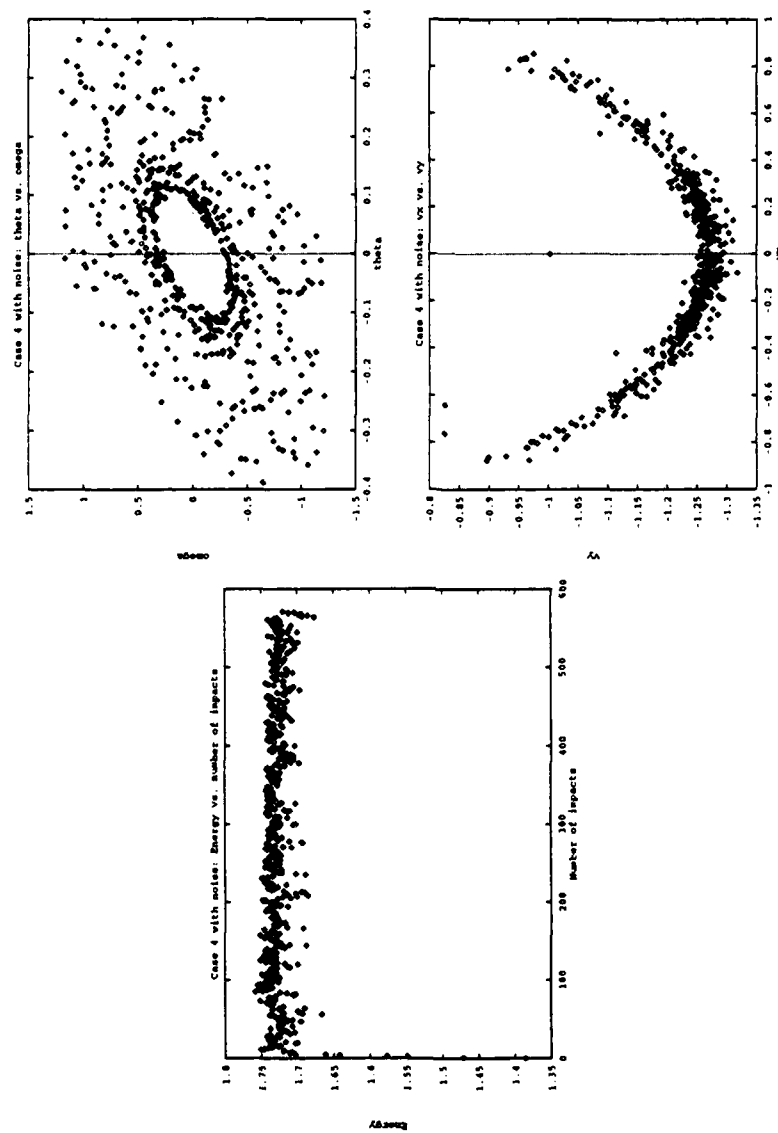
Figure 12: Case 4 with noise

3 Conclusions

The experiments show that, under ideal conditions, control of the object is theoretically possible using knowledge of the collision parameters. The biggest problems are, of course, dealing with friction and setting up the necessary sensing and control. Although indications are that stability can be maintained for reasonably accurate robot and sensors, handling friction will be necessary before this scheme can be considered feasible.

In terms of applicability to other domains, the results may also be useful in the dual problem of planning the acquisition of a stationary object with an accelerating hand, or in catching. For these tasks, we consider the desired stable state to be zero relative velocity (and distance) between the object and the robot hand. Then we would like to plan the movements of the hand so that the object does not fall or bounce away from the hand, but instead eventually settles there. Work on this is underway.

A Appendix: Impact Dynamics

Following [17], the impulse equations for a body of mass m colliding with point contact against a barrier (where it is assumed that $m_{barrier} >> m$) are given by

$$
\begin{aligned}
m(v_t - v_{t0}) &= P_t \\
m(v_n - v_{n0}) &= P_n \\
m\rho^2(\omega - \omega_0) &= P_\omega = P_t l \cos\beta + P_n l \sin\beta
\end{aligned}
\tag{31}
$$

Here, v_t is the relative velocity of the body tangential to the contact normal, and v_n is the component normal to the contact. The subscript 0 designates initial velocity. P_t and P_n are the components of the impulse in the tangential and normal directions, respectively. The velocity of the contact point is given by

$$
\begin{aligned}
v_{tc} &= v_t + l\omega \cos\beta \\
v_{nc} &= v_n + l\omega \sin\beta.
\end{aligned}
\tag{32}
$$

As in Figure 1, β is the angle of the line from the center of gravity of the object to the contact point with respect to the contact normal, in the counterclockwise direction.

Combining (31) with (32) gives us

$$
\begin{aligned}
v_{tc} &= v_{tc0} + \frac{\rho^2 + l^2 \cos^2\beta}{m\rho^2} P_t + \frac{l^2 \sin\beta \cos\beta}{m\rho^2} P_n \\
v_{nc} &= v_{nc0} + \frac{l^2 \sin\beta \cos\beta}{m\rho^2} P_t + \frac{\rho^2 + l^2 \sin^2\beta}{m\rho^2} P_n
\end{aligned}
\tag{33}
$$

24

Newton's model for impact (see [17], [19], or [4]) divides the (normal) impulse into two parts. compression, when the colliding objects are moving into each other, and restitution, when the objects move away from each other. Newton's hypothesis is that the impulse of restitution and the impulse of compression are in the ratio e. We define P_{n0} as the impulse at full compression: that is, when $v_{nc} = 0$. This assumption, plus the assumption of no friction give us the expressions

$$P_t = 0; \quad P_n = (1 + e)P_{n0}. \tag{34}$$

Substituting (34) into (33) gives

$$
\begin{aligned}
P_n &= -(1 + e)\frac{m\rho^2}{\rho^2 + l^2 \sin^2 \beta} v_{nc0} \\
P_w &= -(1 + e)l \sin \beta \frac{m\rho^2}{\rho^2 + l^2 \sin^2 \beta} v_{nc0}.
\end{aligned} \tag{35}
$$

If now we assume (again following Figure 1) that the collision reference frame is oriented at angle α with respect to the horizontal (the x-y frame), and θ is the angle the object makes with the vertical, then $\beta = \theta - \alpha$. If we rotate (35) and (32) into the x-y frame, we will get (using the notation from equation (1))

$$\Delta \mathbf{v} = -(1 + e)\hat{\mathbf{n}}\hat{\mathbf{n}}^T \mathbf{v}^-, \tag{36}$$

from which (1) follows in the lossless ($e = 1$) case. (24) follows as well, if we recall that (36) refers to relative velocity, and that the table velocity is assumed unaffected by the collision.

B Appendix: Linear and Nonlinear Systems

Although the equations for our system are nonlinear, we might hope to gain some understanding of its behavior, at least about $\mathbf{x}^*$, by the linear approximation. Nonlinear systems theory ([3]) tells us that if the linearized approximation is asymptotically stable/unstable (in other words, if $\mathcal{J}(\mathbf{x}^*)$ has no eigenvalues on the unit circle), then the nonlinear system is also asymptotically stable/unstable. This would normally justify our examination of the linearized system. Unfortunately, the system under consideration here always has at least two eigenvalues on the unit circle, so we cannot use this standard argument. However, this system is conservative, and therefore $\mathcal{J}$ has determinant 1. It can be shown ([10], [2]) that the following are true in this case:

1. If λ is an eigenvalue of the system, then λ^*, the complex conjugate, is also an eigenvalue[3].

---

[3] This is always true for a system with real matrix entries.

25

2. If λ is an eigenvalue of the system, then $1/\lambda$ is also an eigenvalue.

Therefore, for a conservative system, stability is only possible if the linear system values are all on the unit circle. The case where the eigenvalues are ± 1 is even more problematic (see [2]), but fortunately in the case at hand, the two complex exponential eigenvalues seem to be the critical values to examine.

C Appendix: The case $\kappa = \kappa_{critical}$

For the case $\kappa = \kappa_{critical}$, $\lambda_{3,4}$ both become 1, and the corresponding eigenvectors both become of the form $[v_{31}, v_{32}, 0, v_{33}]$, $v_{31}, v_{32}, v_{33} \in \Re$. This means that $\mathcal{J}$ is no longer diagonalizable, but contains more general Jordan blocks; in other words, the "generalized eigenvectors" must all satisfy either

$$\mathcal{J}\mathbf{V}_i = \lambda_i \mathbf{V}_i \quad \text{or} \quad \mathcal{J}\mathbf{V}_i = \lambda_i \mathbf{V}_i + \mathbf{V}_{i-1} \qquad (37)$$

([18]). If we find the fourth "eigenvector" and expand our solution, we obtain

$$\delta\mathbf{x}_n = c_1 \begin{bmatrix} 0 \\ 1 \\ 0 \\ 0 \end{bmatrix} + c_2 \begin{bmatrix} 0 \\ 0 \\ 1 \\ 0 \end{bmatrix} + (c_3(-1)^n + nc_4) \begin{bmatrix} V_{31} \\ V_{32} \\ 0 \\ V_{33} \end{bmatrix} + c_4(-1)^n \begin{bmatrix} V_{41} \\ V_{42} \\ 0 \\ V_{43} \end{bmatrix} \qquad (38)$$

which would appear to only be stable for a limited number of initial conditions, at best. However, this case seems to be fairly stable in simulation.

References

[1] Andersson, R. L.; "Understanding and applying a robot ping-pong player's expert controller", *Proceedings of the 1989 IEEE International Conference on Robotics and Automation*, 1989.

[2] Arnold, V. I.; *Mathematical Methods of Classical Mechanics*, Springer-Verlag, New York, 1978.

[3] Arrowsmith, D. K.; Place, C. M.; *Dynamical Systems*, Chapman and Hall, London, 1992.

[4] Brach, Raymond M.; *Mechanical Impact Dynamics*, John Wiley & Sons, New York, 1991.

[5] Bühler, Martin; *Robotic Tasks with Intermittent Dynamics*, Ph.D. Thesis, Yale University, 1990.

[6] Erdmann, M.A; *On Motion Planning with Uncertainty*, M.S. Thesis, MIT, AI-TR-810, 1984.

[7] Goyal, S.; Ruina, A.; Papadopoulos, J.; *Planar Sliding with Dry Friction 1: Limit Surface and Moment Function*, Technical Report 90-1108, Cornell University, 1990.

[8] Goyal, S.; Ruina, A.; Papadopoulos, J.; *Planar Sliding with Dry Friction 2: Dynamics of Motion*, Technical Report 90-1109, Cornell University, 1990.

[9] Koditschek, D.; Bühler, M.; "Analysis of a Simplified Hopping Robot", *International Journal of Robotics Research*, vol. 10, no. 6, December 1991.

[10] Lichtenberg, A. J.; Lieberman, M. A.; *Regular and Stochastic Motion*, Springer-Verlag, New York, 1983.

[11] Lozano-Pérez, T.; "Spatial Planning: A Configuration Space Approach", *IEEE Transactions on Computers*, C-32(2):108-120, 1983.

[12] Lynch, K. ; "The Mechanics of Fine Manipulation by Pushing", *Proceedings of the IEEE International Conference on Robotics and Automation*, 1992.

[13] Mason, M. ; "Mechanics and Planning of Manipulator Pushing Operations", *International Journal of Robotics Research*, vol. 5, no. 3, Fall 1986.

[14] Peshkin, M. A.; "The Motion of a Pushed, Sliding Workpiece", *IEEE Journal of Robotics and Automation*, vol. 4, no. 6, December 1988.

[15] Raibert, M.H.; *Legged Robots that Balance*, The MIT Press, Cambridge, MA, 1986.

[16] Rizzi, A.A.; Koditschek, D.E.; "Progress in Spatial Robot Juggling", *Proceedings of the 1992 IEEE International Conference on Robotics and Automation*, 1992.

[17] Routh, Edward John; *Dynamics of a System of Rigid Bodies, Vol. 1*, Dover Publications, New York, 1960.

[18] Strang, Gilbert; *Linear Algebra and Its Applications*, Academic Press, 1980.

[19] Wang, Yu; *On Impact Dynamics of Robotic Operations*, Technical Report CMU-RI-TR-86-14, Robotics Institute, Carnegie Mellon University, 1986.

[20] Wang, Yu; *Dynamic Analysis and Simulation of Mechanical Systems with Intermittent Constraints*, Ph.D. Thesis, Carnegie Mellon University, 1989.